

# The Anisotropic Wilson Gauge Action

Timothy R. Klassen

SCRI, Florida State University  
Tallahassee, FL 32306-4130, USA

## Abstract

Anisotropic lattices, with a temporal lattice spacing smaller than the spatial one, allow precision Monte Carlo calculations of problems that are difficult to study otherwise: heavy quarks, glueballs, hybrids, and high temperature thermodynamics, for example. We here perform the first step required for such studies with the (quenched) Wilson gauge action, namely, the determination of the renormalized anisotropy  $\xi$  as a function of the bare anisotropy  $\xi_0$  and the coupling. By, essentially, comparing the finite-volume heavy quark potential where the quarks are separated along a spatial direction with that where they are separated along the time direction, we determine the relation between  $\xi$  and  $\xi_0$  to a fraction of 1% for weak and to 1% for strong coupling. We present a simple parameterization of this relation for  $1 \leq \xi \leq 6$  and  $5.5 \leq \beta \leq \infty$ , which incorporates the known one-loop result and reproduces our non-perturbative determinations within errors. Besides solving the problem of how to choose the bare anisotropies if one wants to take the continuum limit at fixed renormalized anisotropy, this parameterization also yields accurate estimates of the derivative  $\partial\xi_0/\partial\xi$  needed in thermodynamic studies.

## 1 Introduction

Lattice QCD has experienced rapid progress in the last few years (see e.g. the proceedings of the latest lattice conference [1]). In particular, it should be viewed as progress that we can now clearly see the limitations of various approximations that have been commonly used in the past, like quenching or the use of (mean-field improved) perturbative coefficients for the improvement terms in actions and currents.

A great theoretical advance in the last two years was the determination of the *non-perturbatively*  $O(a)$  improved Wilson quark action for both quenched [2, 3, 4] and full ( $n_f=2$ ) QCD [5] initiated by the ALPHA collaboration. These results are most relevant for the study of light hadrons. They are therefore only of limited value in the study of heavy quark systems, where we are also beginning to see the limitations of current methods. The most popular of these are the NRQCD [6] and Fermilab [7] approaches.

The problem is, as for the standard Wilson quark action, that the non-perturbative corrections to the  $O(a)$  improvement coefficients in these actions are large on coarse lattices. Different mean-field prescriptions to take some of these corrections into account give quite different results on coarse lattices [8]. A non-perturbative determination of these coefficients is therefore called for.

We think that the most reliable and ultimately simplest approach is to perform the non-perturbative  $O(a)$  improvement *not* for the NRQCD or Fermilab formalisms, but rather to extend the Symanzik improvement program for Wilson-type quark actions to *anisotropic* lattices, with a temporal lattice spacing  $a_t$  much smaller than the spatial one  $a_s$ . On such lattices heavy quarks will not suffer large lattice artifacts as long as their masses are small in units of  $a_t$ . At the expense of the relatively modest cost incurred by simulating a lattice with a larger temporal extent one can study heavy quark systems in a relativistic framework with controlled errors. Such studies would be orders of magnitude more expensive on isotropic lattices. The use of anisotropic lattices for heavy quark physics was advocated in refs. [9, 10, 11]; we refer to [9] for studies of the classical case and to [10] for some exploratory simulations.

Anisotropic lattices are also important in other situations. Generally speaking, they allow one to reap many of the benefits of fine lattices, while still using cheap coarse spatial lattices:

- The signal to noise ratio of correlation functions calculated in Monte Carlo simulations generically decays exponentially in time. Choosing a smaller temporal lattice spacing gives more time slices with an accurate signal, enabling more precise and confident mass determinations, for example. This is crucial for particles with bad signal/noise properties like glueballs [12], hybrids and P-state mesons. For the same reason it is also clear that *excited-state* masses can be determined much more accurately on anisotropic lattices.
- For a full determination of thermodynamic quantities one has to be able to take independent derivatives with respect to temperature and volume. The simplest way to achieve this, is to have independent spatial and temporal lattice spacings. The point of the previous paragraph also becomes important at high temperatures, where one needs a small temporal lattice spacing to have a sufficient number of Matsubara frequencies for accurate studies of the electro-weak phase transition, transport coefficients in the quark-gluon plasma phase, and many other issues.
- By euclidean invariance we can also think of the small lattice spacing as a spatial one. This allows one to study large spatial momenta, which are phenomenologically important for form factors, for example.

Of course, the advantages of anisotropic lattices come at a price, namely, that coefficients in the action have to be tuned to restore space-time exchange symmetry on the quantum level. In the context of the  $O(a)$  improvement program, the good news is that the increase in the number of coefficients that have to be determined for a relativistic action is quite modest: For a Wilson-type quark action there are three (instead of one)

coefficients to be tuned to achieve non-perturbative  $O(a)$  improvement [11]. How to achieve this using the Schrödinger functional, similar to the isotropic case [2], has been outlined in [11].

However, before worrying about the quark action, we have to consider gauge actions on anisotropic lattices. The first step is the study of pure gauge theory, relevant for quenched QCD. In this paper we will consider the simplest case, the anisotropic Wilson gauge action [13, 14].<sup>1</sup> For this action no coefficients have to be tuned to restore space-time exchange symmetry up to  $O(a^2)$  errors. Nevertheless, there is something to be done, since we have to know the true or *renormalized anisotropy*  $\xi \equiv a_s/a_t$  as a function of the bare parameters. This is important, because we would like to take the continuum limit at a fixed value of the renormalized anisotropy, for example.

Our aim in this paper is to develop a simple and accurate method to determine the renormalized anisotropy and apply it to the Wilson plaquette action. For  $SU(N)$  gauge fields we write this action on an anisotropic lattice as

$$S = \frac{\beta}{N} \sum_{x,s>s'} \frac{1}{\xi_0} \text{Re Tr} (1 - P_{ss'}(x)) + \xi_0 \text{Re Tr} (1 - P_{0s}(x)). \quad (1.1)$$

Here  $P_{\mu\nu}(x)$  is the plaquette operator in the  $\mu\nu$ -plane,<sup>2</sup> i.e. the product of link fields around a single plaquette (with  $x$  chosen according to any consistent convention as one of its corners). Expanding the action in terms of the field strength for small lattice spacings, it is easy to see that at the classical level  $\xi_0 = a_s/a_t$ , if we use  $\beta \equiv 2N/g^2$  to introduce the bare coupling  $g$  as in the isotropic case. This justifies the name *bare anisotropy* for  $\xi_0$ .

Our problem is to determine the relation  $\xi = \xi(\xi_0, \beta)$ , or its inverse,  $\xi_0 = \xi_0(\xi, \beta)$ , which is actually preferable from a practical point of view. In sect. 2 we describe the physical ideas behind the “ratio method” we use to determine this relation non-perturbatively. Basically the same method was used previously in [16, 17, 18] (but not always with the same results, as we will see). In sect. 3 we present the details of our implementation of these ideas and of our simulations of the anisotropic  $SU(3)$  plaquette action. Our results cover both fine and coarse lattices and five anisotropies in the range  $1.5 \leq \xi \leq 6$ . In sect. 4 we use known perturbative results to motivate parameterizations that reproduce all our data within errors. We also briefly discuss the application of our results in high precision thermodynamic studies. We conclude in sect. 5 with a summary and an outlook on future work.

---

<sup>1</sup>Determinations of the renormalized anisotropy for improved actions will be reported in [15].

<sup>2</sup>Here a summary of our lattice conventions: We always work on four-dimensional hypercubic lattices with periodic boundary conditions. Directions are labelled by  $\mu = 0, 1, 2, 3$  or  $t, s, s'$ , where  $t=0$  stands for the time and  $s, s'$  for a space direction.  $a_\mu$  is the lattice spacing in direction  $\mu$  (we write  $\mathbf{a}_\mu$  if we want to consider the spacing as a vector in the positive  $\mu$  direction), and we assume spatial isotropy, i.e. that all spatial  $a_\mu$  are the same, equal to  $a_s$ . For the extensions of the lattice we write  $L_\mu$  and  $N_\mu = L_\mu/a_\mu$  in physical and lattice units, respectively.

## 2 Non-Perturbative Determination of the Renormalized Anisotropy

The obvious spectral quantity to extract the renormalized anisotropy  $\xi$  of a gauge action from is the static potential. Actually, on an anisotropic lattice there are *two* potentials, according to whether the heavy quark and anti-quark propagate along the time or a space direction. We will refer to them as the “regular” and “sideways” potential, and denote them by  $V_t(\mathbf{r})$  and  $V_s(\mathbf{r})$ , respectively.

On the lattice  $V_t(\mathbf{r})$  is measured in units of the temporal lattice spacing and  $V_s(\mathbf{r})$  in terms of the spatial one. They therefore differ by a factor of  $\xi$ . However, they also differ by an additive constant, since the self-energy corrections to the static potential are different if the quarks propagate along the time or a space direction. To determine  $\xi$  from a comparison of the regular and sideways potential we therefore have to demand,

$$V_s(\mathbf{r}) \stackrel{!}{=} \xi V_t(\mathbf{r}) + \text{const}, \quad \text{for sufficiently large spatial } \mathbf{r}. \quad (2.1)$$

Note that due to the  $O(a_s^2, a_t^2)$  errors of the potential(s), the above equality will in principle only hold for asymptotically large  $r$ . From experience with the static potential we expect that the components of  $\mathbf{r}$  have to be at least 2 – 3 in units of  $a_s$ , for the systematic  $O(a_s^2, a_t^2)$  errors in  $\xi$  to be below the 1% level.

Due to the constant in (2.1) this approach always requires several  $\mathbf{r}$  values to obtain an estimate of  $\xi$ . Since one cannot use small  $r$  and errors increase rapidly at larger  $r$ , this approach is relatively expensive (and not very elegant, with a complicated error analysis if done properly).

A much better approach involves comparing the sideways potential with the quarks separated along a spatial direction with the case where they are separated along the time direction.<sup>3</sup> There is no additive constant to complicate matters and we can demand

$$V_s(y\mathbf{a}_s) \stackrel{!}{=} V_s(y\xi\mathbf{a}_t) \quad \text{for sufficiently large } y. \quad (2.2)$$

Using one’s favorite method of calculating the static potential one can obtain an estimate of  $\xi$  for each value of  $y$  (on the right hand side one will generically have to interpolate between two values of  $y\xi$ ). The estimated  $\xi$  should rapidly reach a plateau as  $y$  increases.

This method is perfectly fine, in principle and in practice. If  $V_s$  is strictly meant to be the (sideways) static potential with negligible finite-volume effects, it does however have a limitation. Namely, it will be difficult to reach small lattice spacings,<sup>4</sup> where the elimination of finite-volume effects in the potential becomes very expensive. However, the finite-volume potential is also a spectral quantity; if we can arrange the physical extent of the lattice to be the *same* in the spatial and the time directions, then the finite-volume effects in  $V_s(y\mathbf{a}_s)$  and  $V_s(y\xi\mathbf{a}_t)$  should also be the same! (Below we will

<sup>3</sup>We could also allow the separation to have a component along (another) spatial direction.

<sup>4</sup>As briefly mentioned in the introduction, we would like to reach small lattice spacings and make contact with perturbation theory, so that we can present an analytic formula for the relation between  $\xi$  and  $\xi_0$  from weak to strong coupling.

describe one way of getting around the problem of how to choose the size of the lattice to correspond to the same physical extent in all directions without knowing  $\xi$  beforehand.)

So, finite-volume effects should not prevent as from measuring  $\xi$  on fine lattices. The remaining question is if we have a signal for “times” large enough so that ratios of Wilson loops allow us to extract the asymptotic value of the (finite-volume) potential. Actually, this is not necessary. Similarly to the logic that allowed us to work with the finite-volume potential we note the following. If the ratios of Wilson loops that asymptotically would reach  $V_s(y\mathbf{a}_s)$  and  $V_s(y\xi\mathbf{a}_t)$  have the *same* excited-state (i.e. finite-“time”) contributions, we can use these ratios at finite “times” to measure  $\xi$ . In other words, we have to set up a situation where the heavy quark anti-quark states that can be thought of as underlying the spatial and temporal Wilson loops in question correspond to the *same physical state* from a continuum point of view, i.e. when ignoring the usual  $O(a_s^2, a_t^2)$  lattice artifacts.

Before proceeding, let us introduce some notation for ratios of Wilson loops, namely,

$$R_{ss}(x, y) \equiv \frac{W_{ss}(x, y)}{W_{ss}(x+1, y)}, \quad R_{st}(x, t) \equiv \frac{W_{st}(x, t)}{W_{st}(x+1, t)} \quad (2.3)$$

in terms of spatial,  $W_{ss}$ , and temporal,  $W_{st}$ , Wilson loops. To avoid cumbersome notation we here measure  $x, y$  in units of  $a_s$  and  $t$  in units of  $a_t$ . Asymptotically, for large  $x$ , the ratios  $R_{ss}(x, y)$  and  $R_{st}(x, t)$  approach  $\exp[-a_s V_s(y\mathbf{a}_s)]$  and  $\exp[-a_s V_s(t\mathbf{a}_t)]$ , respectively.

For  $R_{ss}$  and  $R_{st}$  to have the same excited-state contribution the spatial and temporal links making up the Wilson loops in (2.3) have to be smeared by the same amount in physical units. A simple way of achieving this is with *no smearing* at all. This leads to the “ratio-of-Wilson-loop” method for determining  $\xi$ , which has been used previously [16, 17, 18].

We will describe our detailed implementation(s) of this method in the next section, where we also provide empirical support for our statements concerning the cancellation of finite “time” and volume effects in  $R_{ss}(x, y)$  and  $R_{st}(x, t)$ .

### 3 Simulation and Results

Let us start by summarizing our discussion of the ratio method in the previous section. Although the ratios of Wilson loops,  $R_{ss}(x, y)$  and  $R_{st}(x, t)$  of eq. (2.3), are *not* spectral quantities (for  $x$  where they can be measured reasonably accurately in practice), we expect excited-state corrections to cancel between them if  $t = \xi y$  and all gauge links are unsmeared. Similarly, finite-volume corrections to  $R_{ss}(x, y)$  and  $R_{st}(x, t)$  are the same if the temporal and spatial extents of the box are equal in physical units, i.e.  $N_t = \xi N_s$  in lattice units. Of course, these statements are expected to hold only if  $x, y$  and  $t$  are not too small; otherwise there can be large  $O(a_s^2, a_t^2)$  lattice artifacts.

The conceptually cleanest way to implement the above ideas in a simulation is to turn the problem around and not measure  $\xi$  for fixed  $\xi_0$ , but rather try to determine the  $\xi_0$  that corresponds to a given  $\xi$ . The following method is simplest if  $\xi$  is an integer, so the reader might want to have this case in mind for the moment.

- For fixed  $\beta$  and  $\xi$  choose a lattice volume  $N_s^3 \times N_t$  with  $N_t = \xi N_s$  and calculate

$$\delta(x, y) \equiv \delta(x, y|\xi) \equiv \delta(x, y; t = \xi y), \quad \text{where} \quad \delta(x, y; t) \equiv \frac{R_{ss}(x, y)}{R_{st}(x, t)} - 1, \quad (3.1)$$

for two or three trial values of  $\xi_0$ .

- Interpolate in  $\xi_0$  to find the zero-crossing of  $\delta(x, y)$  for fixed  $x, y$ . This determines an estimate of the non-perturbative  $\xi_0(\xi, \beta)$  for the given  $x, y$ .
- Consider different  $x, y$ ; look for a plateau of  $\xi_0(\xi, \beta)$  as  $x$  and  $y$  increase.

By starting at weak coupling, where perturbation theory can be used, and working one's way towards large coupling it is relatively easy to estimate trial values of  $\xi_0$  that bracket the correct  $\xi_0(\xi, \beta)$  quite closely. In almost all cases we only needed two trial values for  $\xi_0$ . The cases where simulations were performed at more than two values were used to check that the  $\delta(x, y)$  are sufficiently linear as functions of  $\xi_0$  over the regions we typically had to interpolate.

We are mainly interested in integer  $\xi$  for which the above method is best suited. However, there is no problem in using it also for "small fractions". For example, one case we investigated somewhat is  $\xi = \frac{3}{2}$ . For even  $N_s$  almost everything goes through as above; the only change is that for  $\delta(x, y = 3)$ , for example, one has to perform an interpolation of  $\delta(x, y = 3; t = 4)$  and  $\delta(x, y = 3; t = 5)$  to  $t = \xi \cdot y = 4.5$ .

As remarked earlier, the above method is perhaps the conceptually cleanest way to proceed, since we choose  $\xi$  not  $\xi_0$  from the start and can therefore make sure that  $L_s = L_t$  in physical units. It was our method of choice for all but the coarsest lattices. However, on the coarsest lattices, where one needs at least 1000 configurations to measure  $\xi_0(\xi)$  with some accuracy, one would like to avoid having to do independent simulations at two or more trial values of  $\xi_0$  (on fine lattices one only needs a few hundred configurations, so this is not such an important issue). This can be achieved with a slightly modified procedure:

- Given a good guess for the value of  $\xi_0$  corresponding to the desired  $\xi$ , calculate  $R_{ss}(x, y)$  and  $R_{st}(x, t)$  by simulation at  $\xi_0$  on an  $N_s^3 \times N_t$  lattice with  $N_t = \xi N_s$ .
- For given  $x, y$  interpolate  $R_{st}(x, t)$  in  $t$  to match  $R_{ss}(x, y)$ . Estimate  $\xi$  as  $\xi = t/y$ .
- Find the plateau of the estimated  $\xi$  as  $x$  and  $y$  increase.

As long as our estimate of  $\xi_0$  was not too bad, all our previous remarks about the cancellation of finite volume effects and such should apply. In this method we obtain  $\xi(\xi_0, \beta)$ , which can be translated into an estimate of  $\xi_0(\xi, \beta)$  at the desired nearby  $\xi$ . We have explicitly checked in a few cases that both methods give consistent results.

We performed simulations at a large set of couplings aiming at  $\xi = 2, 3, 4$  and a smaller set for  $\xi = 1.5, 6$ . We generated between a few hundred and up to 2700 (almost) independent configurations at weak, respectively, strong coupling. We used two sets of

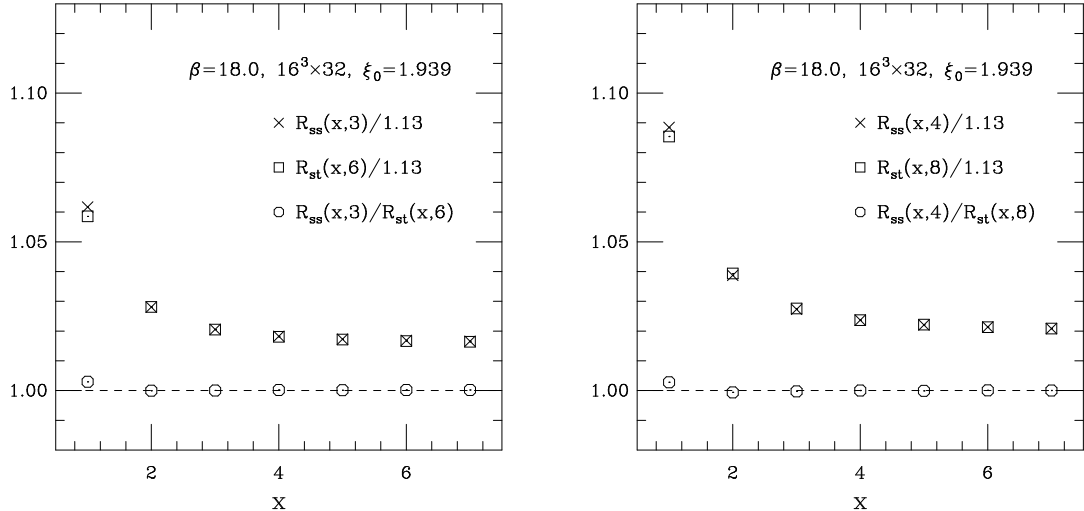


Figure 1: Ratios  $R_{ss}(x, y)$ ,  $R_{st}(x, t)$  and the “ratios of ratios”  $R_{ss}(x, y)/R_{st}(x, t = \xi y)$  as functions of  $x$  for fixed  $y, t$  for a very fine lattice,  $\beta = 18$ ,  $\xi \approx 2$ . Shown are  $y = 3$  (left) and  $y = 4$  (right). The  $R_{ss}(x, y)$  and  $R_{st}(x, t)$  have been rescaled by some overall factor simply so that they can be put more meaningfully on the same plot with their ratio.

code. One employs Metropolis, the other Kennedy-Pendleton [19] heatbath updating; in both cases alternating with microcanonical over-relaxation steps [20].

We started at weak coupling where our method worked so well that we initially did not use link integration [21] for Wilson loops. On coarse lattices, however, fluctuations are large and link integration yields a large saving in CPU time. It was implemented by replacing independent links in a Wilson loop by their average over 20 local updates at fixed values of the staples surrounding the given link.

Most simulations were performed on lattices with  $N_s = 8$  or 10. In several cases we also ran at  $N_s = 12, 16$ , with otherwise the same parameters, and found no significant difference from the results on smaller volumes. This is in accord with the theoretical expectations discussed earlier.

We performed one fine, one intermediate, and one coarse lattice simulation with  $N_s = 16$ , generating about the same number of configurations as for the smaller volumes (we used three trial values of  $\xi_0$  for the fine lattice, two for the others). The errors of these results are therefore quite small; they were used to investigate the question of when  $\xi_0(\xi)$  determined from different  $\delta(x, y)$  reaches its plateau as  $x$  and  $y$  increase. If we can show that the plateau is reached quite early, we can then confidently determine it with less statistics in other cases.

First of all, we should point out the obvious, namely that the existence of a “plateau” depends on the accuracy requested; if one demands infinite precision, the plateau would of course only be reached as  $x, y \rightarrow \infty$ . Our aim is to determine the relation between  $\xi$  and  $\xi_0$  to about 1%. Let us now investigate when a plateau of this accuracy is reached.

In figures 1 – 3 we show the ratios  $R_{ss}(x, y)$  and  $R_{st}(x, t)$  and their “ratio of ratios”

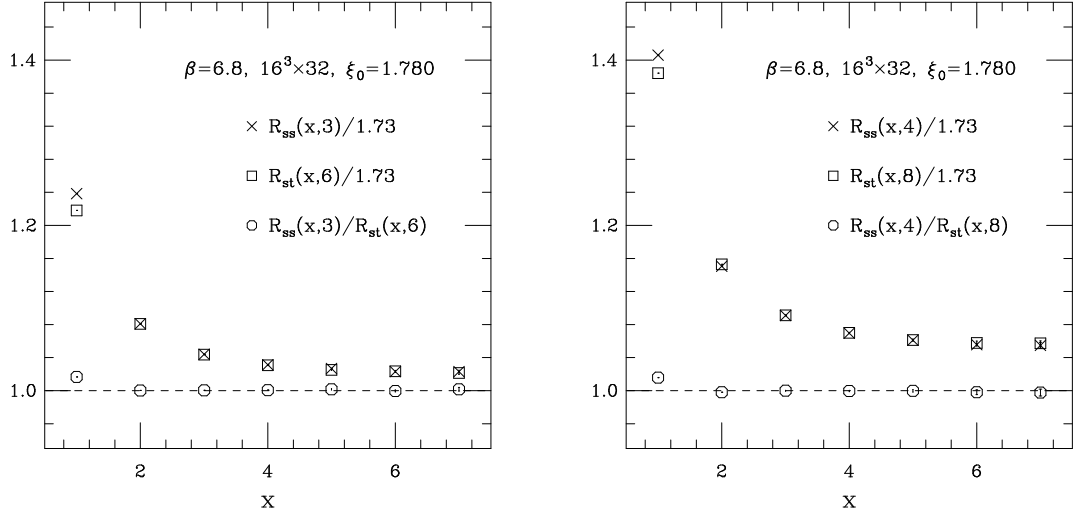


Figure 2: As in figure 1 for an intermediate coupling,  $\beta = 6.8$ ,  $\xi \approx 2$ .

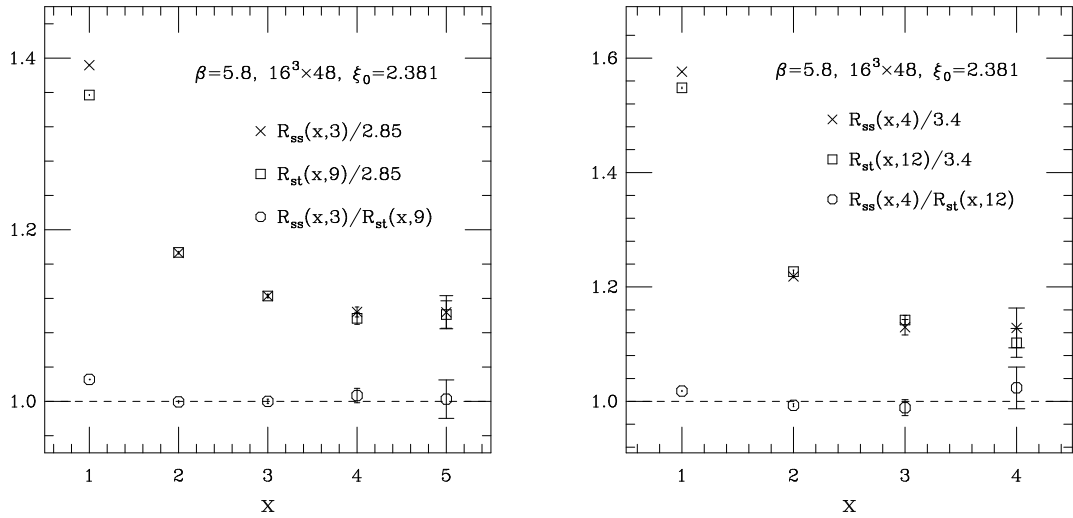


Figure 3: As in figure 1 for a coarse lattice,  $\beta = 5.8$ ,  $\xi \approx 3$ .



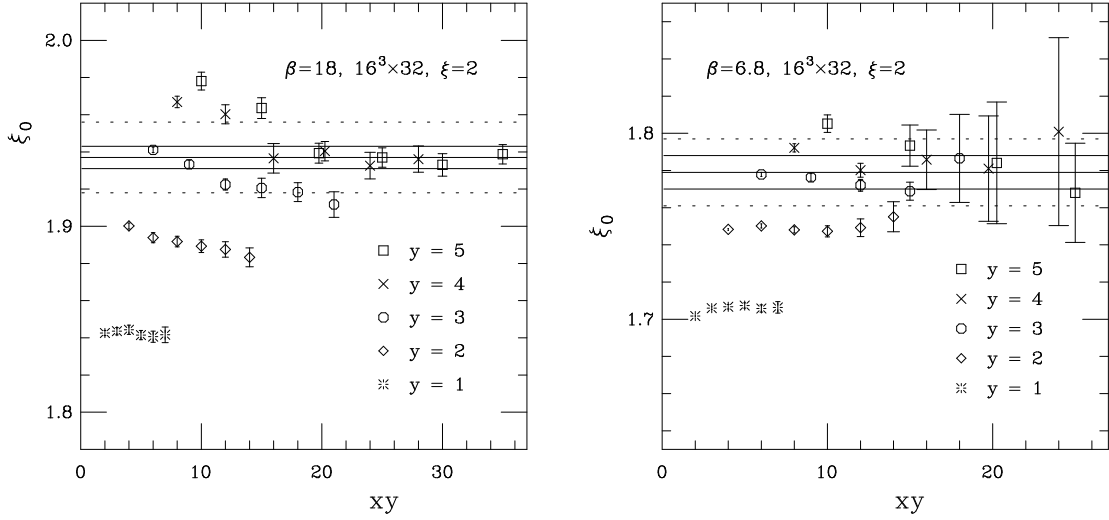


Figure 4:  $\xi_0$  estimated from different (ratios of) Wilson loops plotted versus the area of the Wilson loops. We show results for a very fine (left) and an intermediate (right) lattice. Separate symbols are used to denote results from different  $y$ . The solid lines are used to indicate our final estimate of  $\xi_0$  and its error. The short-dashed lines denote a 1% band around the estimated  $\xi_0$ . Points that would otherwise overlap have been slightly separated. For details see the main text.

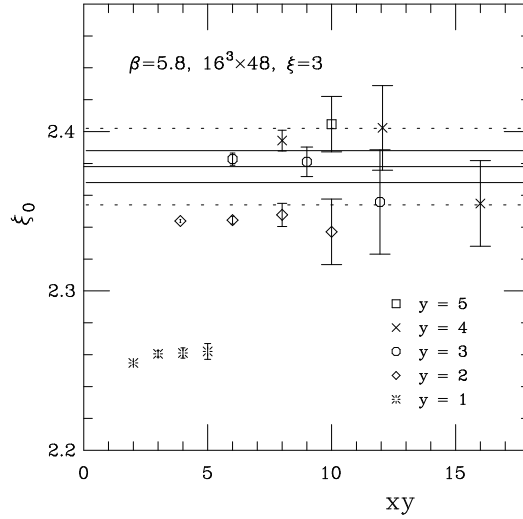


Figure 5: As in figure 4 for a coarse lattice,  $\beta = 5.8, \xi = 3$ .

$\xi$	$\beta$	$\eta$
1.5	5.6	1.1462(114)
	6.3	1.0981(48)
	8.0	1.0631(43)
	24.0	1.0183(35)
2.0	5.4	1.2658(184)
	5.5	1.2560(117)
	5.6	1.2203(112)
	5.8	1.1905(92)
	6.3	1.1527(33)
	6.8	1.1242(51)
	8.0	1.0941(30)
	12.0	1.0515(44)
	18.0	1.0325(32)
	24.0	1.0214(26)
3.0	5.5	1.3351(134)
	5.6	1.3043(130)
	5.8	1.2616(53)
	6.3	1.1947(38)
	6.8	1.1650(36)
	8.0	1.1186(33)
	12.0	1.0676(30)
	24.0	1.0288(18)
4.0	5.4	1.4126(245)
	5.5	1.3652(137)
	5.6	1.3374(94)
	5.8	1.2887(71)
	6.3	1.2162(67)
	6.8	1.1894(39)
	8.0	1.1328(45)
	9.5	1.1056(40)
	12.0	1.0735(32)
6.0	24.0	1.0333(16)
	5.6	1.3738(114)
	6.3	1.2434(104)

Table 1: Simulation results for the renormalization of the anisotropy,  $\eta = \xi/\xi_0$ .

$R_{ss}(x, y)/R_{st}(x, t)$  as a function of  $x$  for two different values of  $y$ . Clearly, excited-state contributions cancel in the ratio of ratios long before the individual ratios reach their plateaux in  $x$  (in fact, it is not clear if they ever do for the unsmeared Wilson loops and volumes we use). This is in accord with expectations discussed earlier. More quantitatively, it seems that  $\delta(x, y)$  reaches its fixed- $y$  plateau to high precision when  $x \geq \max(y-1, 2)$ . With somewhat less accuracy the plateau is apparently already reached for  $x=2$ , even for  $y \geq 4$ , at least for not too fine lattices.

Concerning the plateau of  $\xi_0(\xi)$  consider figures 4 and 5, where the values determined from different Wilson loops are presented. For fixed  $y$  we see the plateau emerging for  $x \geq \max(y-1, 2)$ . It seems that  $y=3$  is sufficient to reach the asymptotic plateau of  $\xi_0$  within the accuracy of interest. In fact, these and other results indicate that the plateau can be obtained to 1% or better from just  $\delta(2, 3)$  and  $\delta(3, 3)$ .<sup>5</sup> In all cases the value so obtained is consistent with that from  $y > 3$  and  $x \geq y - 1$ . Of course, at strong coupling the errors rise so rapidly as  $x, y$  increase, that it is next to impossible to show with the same confidence and accuracy as on finer lattices that a plateau has been reached. However, within the stated aim of 1% errors our simulations results indicate that this is the case. This is also plausible a priori, since  $x, y = 3$ , say, which on fine lattices clearly gives results within 0.5% or so of the asymptotic value, corresponds to a *much* larger distance in physical units on coarse lattices.

The final values we quote for  $\xi_0(\xi)$  were obtained by not just considering results from fixed  $x, y$  (as in the figures above) but also *sums* of Wilson loops: We sum  $\delta(x, y)$  over various  $x, y$  satisfying  $y \geq 3$ ,  $x \geq y - 1$  and then find the zero crossing in  $\xi_0$ . Larger sums were considered for fine lattices, smaller ones for coarse lattices. This was mainly done to minimize the subjective element in choosing the final  $\xi_0(\xi)$ . For the errors, on the other hand, we were rather conservative and take into account the scatter observed between different (sums of) Wilson loops.

Errors of the individual  $\delta(x, y)$  or sums thereof (and of  $\xi = t/y$  in the second method) were evaluated with the bootstrap method using 100 bootstrap ensembles. Before bootstrapping, the data were binned to check for auto-correlations (and save disk space). We always found that errors were stable, at least after some initial binning had been performed. Our final results are shown in table 1, where we present the measured *renormalization of the anisotropy*,  $\eta \equiv \xi/\xi_0$ .

Concerning the conceptual underpinnings of our method we should remark that we have investigated in one case what happens if one uses *smeared* Wilson loops. With no effort to tune the smearing to be the the same in physical units (however one may want to define this) when the (imaginary) heavy quarks are separated along a spatial or the temporal direction, we find that the individual ratios  $R_{ss}(x, y)$  and  $R_{st}(x, t)$  reach their plateaux earlier, as expected, but their ratio reaches its plateau *later* than without smearing. This demonstrates that there is indeed a cancellation of excited-state contributions in the “ratio of ratios” of unsmeared Wilson loops.

---

<sup>5</sup>For fine lattices the  $\xi_0$  determined from  $\delta(x, 3)$  for large  $x > 3$  might be just on the boundary of the 1% band around the asymptotic value we are aiming for. However, it would appear that the  $\xi_0$  from  $x = 2, 3$  are well within the 1% band, as figures 4 and 5 and all our other results indicate.

## 4 Parameterizing the Renormalization of the Anisotropy

For future use in simulations we would like to present analytic parameterizations of the results obtained in the previous section. Given a good parameterization it is guaranteed that observables calculated with the anisotropic Wilson action extrapolate smoothly, like  $a^2$  asymptotically, to the continuum limit. If we had performed simulations at the central values of the measured  $\xi_0(\xi, g^2)$  of the previous section, data obtained from runs with sufficiently high statistics would *not* lie on a smooth curve. Furthermore, a good parameterization allows us to perform simulations at any coupling, not just the ones we happened to use in sect. 3.

### 4.1 The $g^2$ dependence of $\eta$

Obviously, a parameterization should be consistent with known perturbative results. The one-loop result for the renormalization of the anisotropy  $\eta$  of the Wilson gauge action was obtained long ago by Karsch [13] (cf. also [22]). At one loop  $\eta$  can be written as, for  $SU(N)$ ,

$$\eta = \eta(\xi_0, g^2) = 1 + \frac{\eta_1(\xi_0)}{2N} g^2 + O(g^4), \quad (4.1)$$

with  $\eta_1(1)=0$  and  $\eta_1(\xi_0)$  increasing monotonically to some finite value in the Hamiltonian limit  $\xi_0 \rightarrow \infty$  (explicit numerical values for the  $\eta_1(\xi_0)$  will be given below). Note that to one-loop order we can replace  $\xi_0$  by  $\xi$  in this equation. We can therefore incorporate the known one-loop coefficients  $\eta_1$  into a fit of the results of sect. 3 for fixed  $\xi$ .

We find that excellent fits of  $\eta(g^2)$  for fixed  $\xi$  are possible to Pade ansätze of the form

$$\eta(g^2) = \frac{1 + c_1 g^2 + c_2 g^4}{1 + c_0 g^2}, \quad (4.2)$$

with  $c_1 - c_0$  constrained to be consistent with one-loop perturbation theory, i.e. equal to  $\eta_1(\xi)/6$ . The coefficients of parameterizations obtained from fits to such ansätze are given in table 2, and a graphic presentation of the  $\xi = 2$  and 4 results is exhibited in figure 6. In these and later plots “boosted 1-loop perturbation theory” refers to the replacement of the bare coupling  $g^2$  by the “boosted” coupling [23, 24]

$$\tilde{g}^2 = \frac{g^2}{\sqrt{W_{ss}(1,1)W_{st}(1,1)}}. \quad (4.3)$$

A more proper mean-field estimate would require [24] an estimate of the appropriate scale for  $\eta$ , which presumably is much more infra-red than that of the naive boosted coupling  $\tilde{g}^2$ . This would lead to better agreement with our non-perturbative determination at strong coupling.

### 4.2 The $\xi$ dependence of $\eta$

We are also interested in parameterizing our results for  $\eta$  as a function of  $\xi$  for fixed  $\beta$ , or, more generally, as a function of both  $\xi$  and  $\beta$ . To obtain an idea of how to proceed

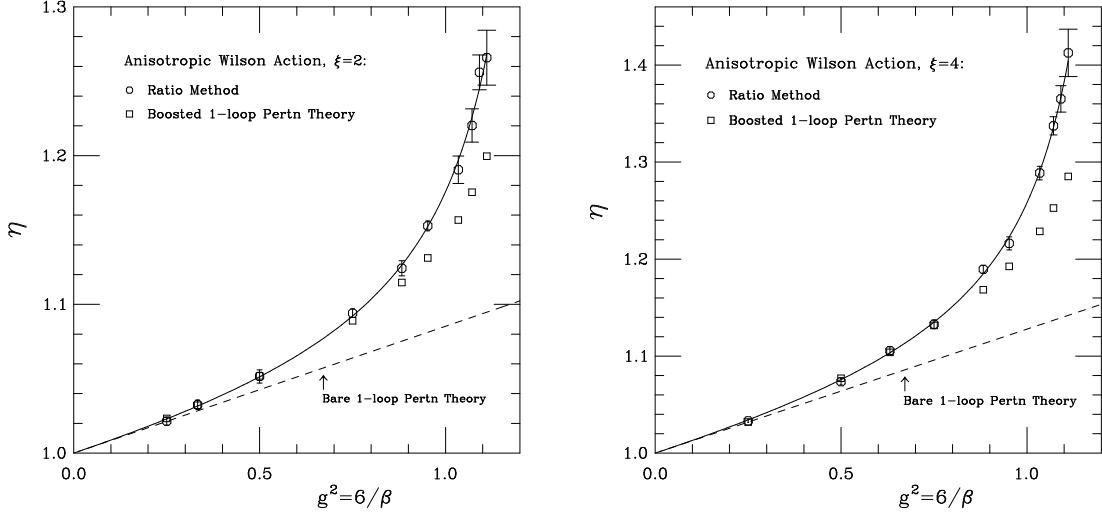


Figure 6: Simulation results and fits of the renormalization of the anisotropy,  $\eta$ , for fixed  $\xi=2$  (left) and  $\xi=4$  (right). For details see the main text.

$\xi$	$c_0$	$c_1$	$c_2$
2.0	-0.76216	-0.67686	-0.04351
3.0	-0.79245	-0.67854	-0.06625
4.0	-0.77715	-0.64925	-0.07038

Table 2: Coefficients of the parameterizations of  $\eta$  at fixed  $\xi$ , eq. (4.2).

let us consider what perturbation theory has to say about the  $\xi$  dependence. A plot of  $\xi$  versus  $\xi_0$  at one-loop using (4.1) and the numerical values of  $\eta_1(\xi_0)$  from [13] and [22] reveals that this relation is amazingly linear, even at large coupling. Rewriting (4.1) as

$$\xi = \eta \xi_0 = \xi_0 + (\xi_0 - 1) \frac{\hat{\eta}_1(\xi_0)}{2N} g^2 + O(g^4), \quad \hat{\eta}_1(\xi_0) \equiv \frac{\xi_0}{\xi_0 - 1} \eta_1(\xi_0), \quad (4.4)$$

shows that this is equivalent to a very weak  $\xi_0$  dependence of  $\hat{\eta}_1(\xi_0)$ . This is indeed the case, as can be seen in table 3.

The main  $\xi_0$  dependence of the one-loop result is taken care of by rewriting  $\eta_1(\xi_0)$  in terms of  $\hat{\eta}_1(\xi_0)$ . We have tried to parameterize the remainder by fitting  $\hat{\eta}_1(\xi_0)$  to a Pade ansatz. We find that the results in table 3 can be represented by

$$\hat{\eta}_1(\xi_0) = \frac{1.002503 + 0.39100 y + 1.47130 y^2 - 0.19231 y^3}{1 + 0.26287 y + 1.59008 y^2 - 0.18224 y^3}, \quad y \equiv \frac{1}{\xi_0}. \quad (4.5)$$

This curve reproduces the numbers in table 3 with an accuracy of about  $10^{-6}$ , which should be sufficient for all practical purposes.

$\xi_0$	$\hat{\eta}_1(\xi_0)$
1.00	1.00068(6)
1.25	1.01116256
1.50	1.01758914
1.75	1.02143638
2.00	1.02364467
2.25	1.02480746
3.00	1.02516137
4.00	1.02319237
5.00	1.02090024
6.00	1.01886792
7.00	1.01716124
8.00	1.01574032
10.00	1.01354821
20.00	1.00846625
$\infty$	1.00250290

Table 3: One-loop coefficient of  $\eta$  for the Wilson gauge action (see eqs. (4.4) and (4.1) for the precise definition of  $\hat{\eta}_1$ ). The  $\xi_0=1$  result is from [13]. All other values are from [22]; they should be accurate to the precision shown.

We can now try to find a representation of all data for  $\eta$ . The most naive hope would be that an ansatz of the form

$$\eta(\xi, g^2) = 1 + \left(1 - \frac{1}{\xi}\right) \frac{\hat{\eta}_1(\xi)}{6} \frac{1 + a_1 g^2}{1 + a_0 g^2} g^2, \quad (4.6)$$

might be adequate. We find that this ansatz is not only adequate but provides a nearly perfect representation of all data in table 1 for  $a_0 = -0.77810$  and  $a_1 = -0.55055$  (the confidence level  $Q$  of a fit is above 0.99, suggesting that our error estimates in sect. 3 were indeed rather conservative). It is quite remarkable that all our simulation results can be summarized with just two fit parameters.

Cross sections of the function (4.6) for fixed  $\xi$  and fixed  $\beta$  can be found in figures 7 and 8, respectively. Since there seems to be no systematic trend in the tiny deviations of the curves from the data, we recommend the use of (4.6) for future applications of the anisotropic Wilson action with  $1 \leq \xi \leq 6$  (instead of the fixed- $\xi$  representations discussed in the previous subsection).

There is one interesting point concerning the  $\xi$  dependence of eq. (4.6) that we should mention. Recall that in one-loop perturbation theory  $\xi$  is a linear function of  $\xi_0$  to high accuracy. The same is therefore true for  $\xi_0$  as a function of  $\xi$ . One might think that the accuracy of the ansatz (4.6) means that the same is true beyond the one-loop level. However, this is not the case. Trying to fit  $\xi_0$  as a linear function of  $\xi$  for fixed  $\beta$  usually leads to very small confidence levels (as low as 0.0005) for  $\beta \leq 8.0$ , whereas quadratic fits

always work very well.<sup>6</sup> The non-linearity can be seen in figure 9 — at least with the help of a ruler — where we plot  $\xi_0$  versus  $\xi$  for several  $\beta$ . This might sound paradoxical at first, but the reason is that  $\xi$  appears on the right hand side of (4.6), not  $\xi_0$ , which might be considered the natural variable in perturbation theory (though it does not matter on the one-loop level).

First of all, the  $\xi$  or  $\xi_0$  dependence of  $\hat{\eta}_1$  is *not* the problem; it is much too weak. The ansatz (4.6) works just as well if we replace  $\hat{\eta}_1$  by 1.02, say. So we can write (4.6) as  $\eta(\xi) = 1 + bz$ , where  $z = (\xi - 1)/\xi$  to a good approximation, and  $b = b(g)$ . This implies  $\xi_0 = \xi/\eta = \xi(1 - bz + b^2z^2 + \dots)$ . Our above finding concerning fits of  $\xi_0(\xi)$  therefore essentially means this: a “quadratic term” (cf. the previous footnote) is present, but within errors it is indistinguishable from the term  $b^2z^2$  that arises from expanding  $1/\eta$ . It is therefore simpler and much better to fit the  $\xi$  dependence of  $\eta$  as in (4.6) instead of fitting  $\xi_0(\xi)$  to a quadratic ansatz (equivalently, one can fit  $\xi_0(\xi)$  to the ansatz  $\xi_0 = \xi/\eta$  with  $\eta$  as above).

To summarize, the non-perturbative  $\xi$  dependence of  $\eta$  is within our errors simply given by replacing  $\xi_0$  by  $\xi$  in the one-loop formula. Why this should be, we do not know, but we are certainly happy to exploit this fact in presenting the simple parameterization (4.6) of all our data.

### 4.3 The derivative $\partial\xi_0/\partial\xi$

Among the immediate applications of this result we would like to point out just one, related to thermodynamic studies. Obtaining all thermodynamic information requires one to take independent derivatives of the partition function with respect to temperature and volume. Even if one is ultimately interested the isotropic case, the most natural way to take these derivatives is to introduce an anisotropic lattice with independent temporal and spatial lattice spacings at an intermediate stage. In addition to the  $\beta$ -function for the dependence of the lattice spacing on the coupling, one needs  $\partial\xi_0/\partial\xi$  to calculate all thermodynamic quantities (for details on lattice thermodynamics see e.g. [25, 26]).

From eq. (4.6) one obtains

$$\frac{\partial\xi_0}{\partial\xi}(\xi=1, g^2) = 1 - \frac{\hat{\eta}_1(1)}{6} \frac{1 + a_1 g^2}{1 + a_0 g^2} g^2 \equiv 1 - \gamma(g) g^2. \quad (4.7)$$

Our  $\gamma(g)$  is shown in figure 10 together with results from a different non-perturbative determination using the “integration of plaquettes” technique [25, 26] (we took the data from table 3 in [26]). This technique can not be used on very coarse lattices and becomes very costly on fine lattices. We therefore only have results for  $5.7 \leq \beta \leq 7.2$  to compare with. No errors are quoted in [26] for these results, but we tried to estimate them from figure 1 in [17] (the same information can be found with higher resolution in figure 5.3 of ref. [18], for example). This error estimate is included in figure 10 for a few points. For our results we also include errors, which were obtained conservatively from fits of  $\eta$

---

<sup>6</sup>To insure that the ansatz for  $\eta$  is well-behaved in the Hamiltonian limit, one might prefer to mean  $\xi_0 = \xi + b_1(\xi - 1) + b_2(\xi - 1)^2/\xi$  by “quadratic ansatz”, instead of the naive  $\xi_0 = \xi + b_1(\xi - 1) + b_2(\xi - 1)^2$ . However, this is not important here; either ansatz works fine for our limited range of  $\xi$ .

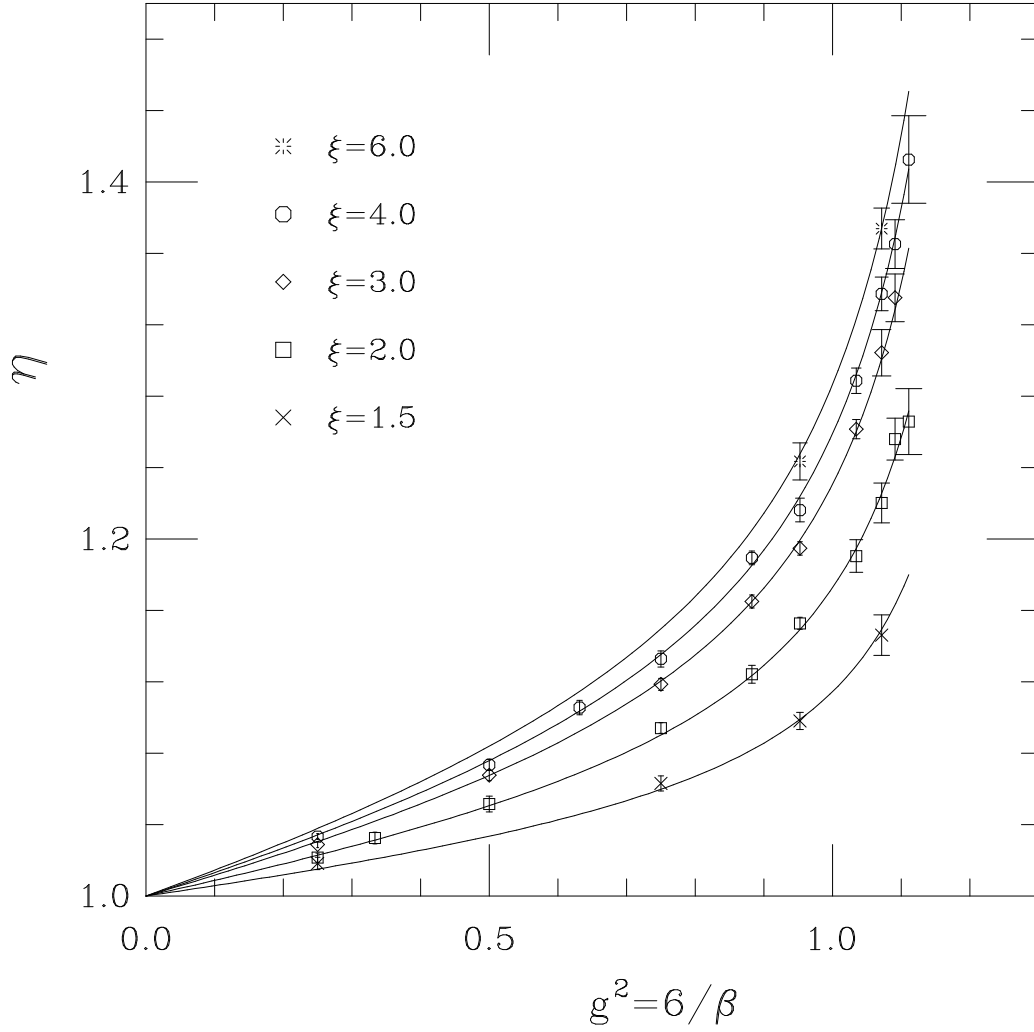


Figure 7: Fixed- $\xi$  cross-sections of our simulation results and the global fit (4.6) for the renormalization of the anisotropy,  $\eta = \xi/\xi_0$ . We show our fit up to  $\beta = 5.4$ .



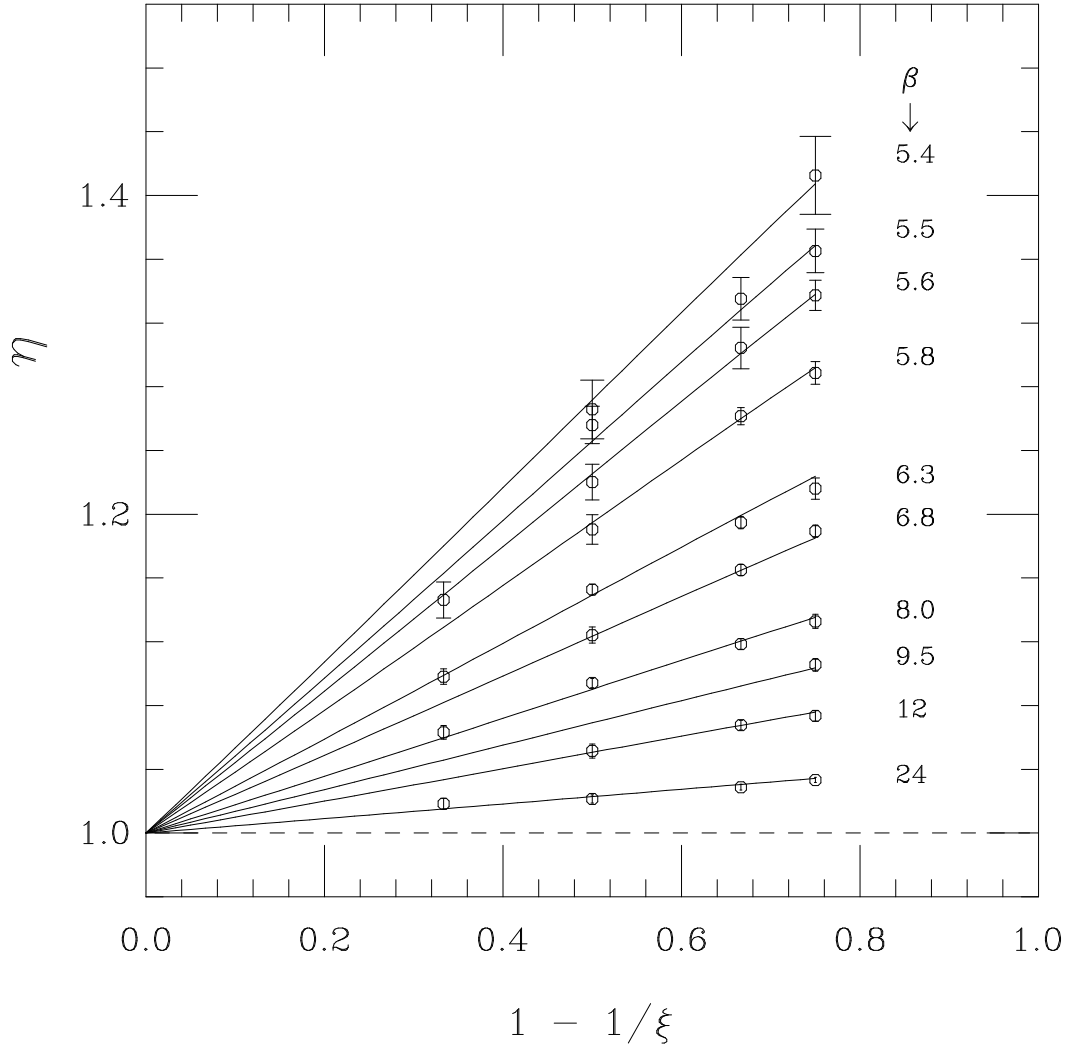


Figure 8: As in figure 7, but now for fixed- $\beta$  cross sections. For fixed  $\beta$  the renormalization of the anisotropy  $\eta$  appears to be an essentially linear function of  $1 - 1/\xi$ , even on coarse lattices.

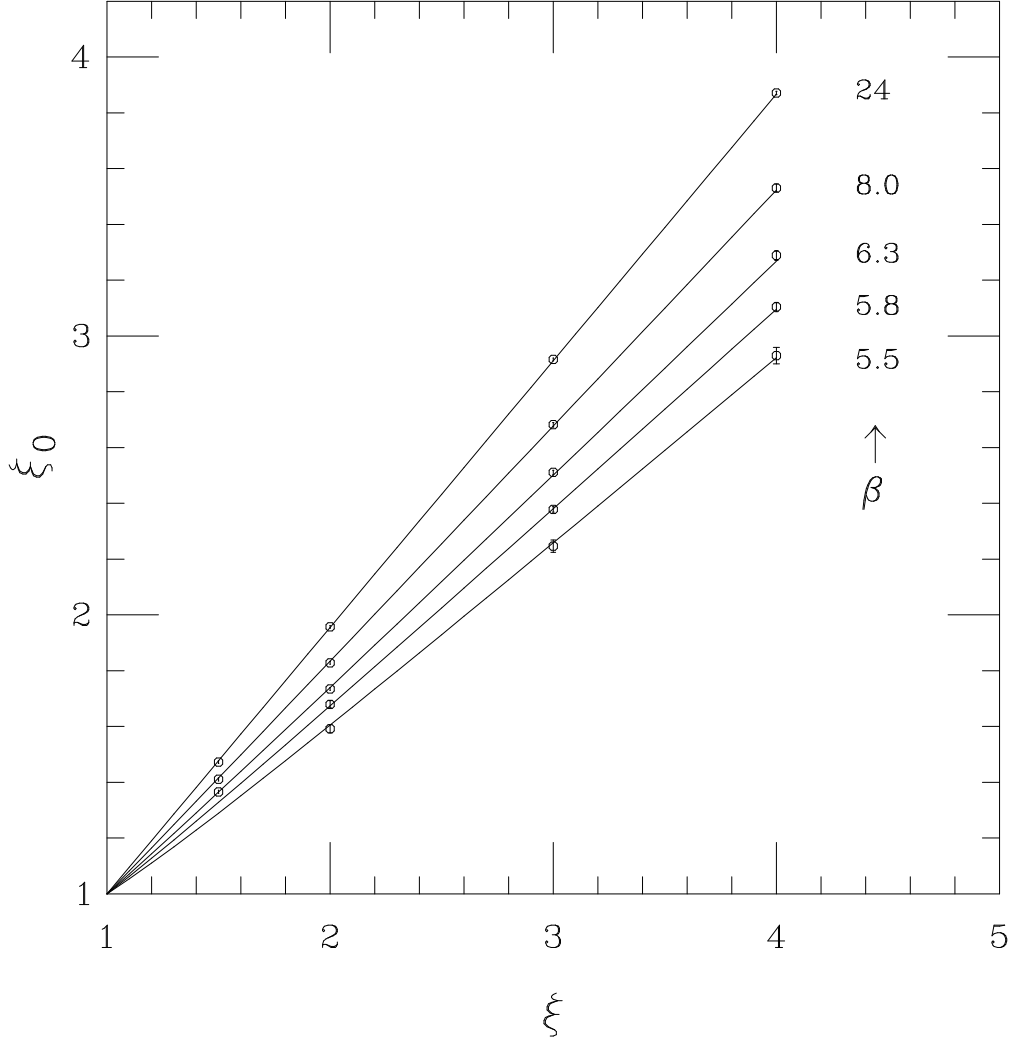


Figure 9: Similar to figure 8, but now we plot the bare versus the renormalized anisotropy (for clarity we only show a subset of the  $\beta$  values we simulated). In this case deviations from linearity are significant within our errors. For details see the main text.

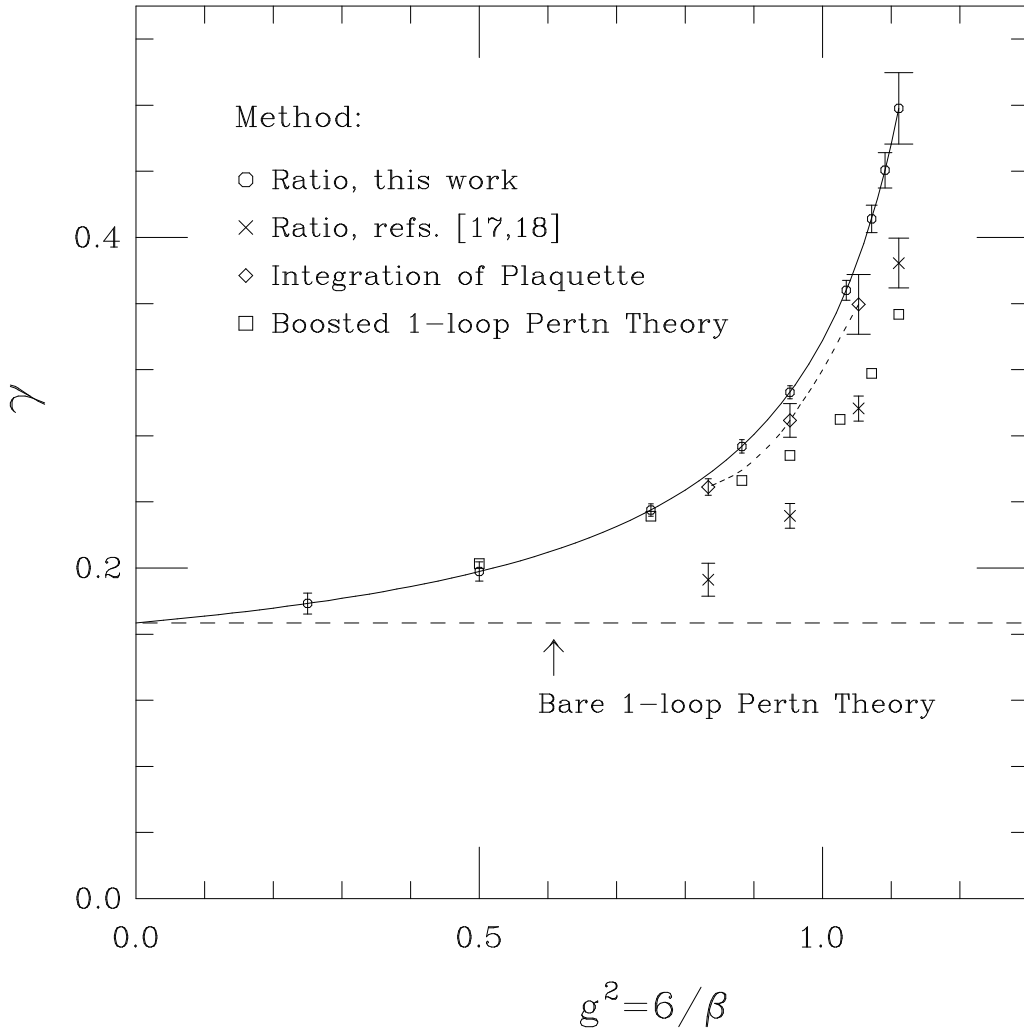


Figure 10: Comparison of non-perturbative determinations of  $\gamma \equiv (1 - \partial\xi_0/\partial\xi)/g^2$  at  $\xi = 1$ . The solid line denotes our result, eq. (4.7), for  $\beta \geq 5.4$ , the short-dashed line is the result from the integration of plaquette technique. The errors of the two methods are shown at several points. We also show results ( $\times$ ) from a previous application of (a version of the) ratio method, which gave rather different results.

versus  $\xi$  at *fixed*  $\beta$ , instead of from our global fit (4.6) (to be sure, the *central values* of our points in figure 10 are from (4.7)).

Considering that different non-perturbative methods can differ by  $O(a^2)$  lattice artifacts, the agreement between the two methods in figure 10 is excellent. On the other hand, neither of these results agrees very well with estimates from a different application of the ratio method [17, 18], which is also shown in figure 10. For the largest  $\beta$  considered these results also appear to be in conflict with boosted perturbation theory. (Our results here and other results [2, 3, 4] have so far always shown boosted perturbation theory to agree quite well with non-perturbative determinations for  $\beta \geq 7$  or so.) The reason for this disagreement is not completely clear.<sup>7</sup>

We should mention that in the SU(2) case the integration of plaquette technique [27] and a different non-perturbative method [28] also agree reasonably well (the latter giving slightly larger  $\gamma(g)$ ), and are far above the perturbative result. Qualitatively the situation is therefore the same as with our SU(3) results.

Using (4.7) and the  $\beta$ -function that can be obtained from the accurate scale determinations for the isotropic Wilson gauge action in [29] (and references therein), all ingredients required for high precision thermodynamic studies with this action are now known for all lattice spacings. Once the string tension and/or Sommer scale  $r_0$  has been determined for the anisotropic Wilson actions, the same will hold for these actions. Lattice artifacts in the thermodynamics of the anisotropic Wilson (gauge or quark) action are considerably smaller [30, 31] than for the isotropic case, so it might be interesting to pursue such studies on anisotropic lattices.

## 5 Conclusion and Outlook

Using a method based on ratios of Wilson loops we have presented an accurate, non-perturbative determination of the relation between the bare ( $\xi_0$ ) and renormalized ( $\xi$ ) anisotropies of the Wilson gauge action. We have argued that these ratios should be thought of as the “finite-volume static potential with excited-state contributions”. By creating the same physical situation with the heavy quarks separated either along a spatial or a temporal direction there should be no significant finite-volume or excited-state corrections to the relation between  $\xi_0$  and  $\xi$  even for moderately small Wilson loops. We have explicitly seen this in our simulations. This fact makes our method quite cheap. Nothing in our method is specific to the Wilson action, so it can also be applied to improved gauge actions.

---

<sup>7</sup>The most likely reason is this: In [17, 18] the ratios  $R_{ss}(x, y)$  and  $R_{st}(x, \xi y)$  were not exactly matched, but rather were allowed to differ by an overall factor (the same for all ratios) that was then fitted and typically came out a few percent above 1 (unfortunately no errors were quoted for this factor in [18]). From our data we can extract the effect that the deviation of this factor (our “ratio of ratios”) from its correct asymptotic value 1 has on the final  $\eta(\xi, g^2)$ . It turns out that it is sufficient to explain the quantitative differences between our and the results in [17, 18]. In particular, for fine lattices  $\eta(\xi, g^2)$  becomes rapidly more sensitive to deviations of the ratio of ratios from 1, providing an explanation for the fact that the difference between our and the results of [17, 18] in figure 10 *increases* rather than decreases for small coupling, contrary to naive expectations.

Our results for  $\xi_0(\xi, g^2)$  are significantly more accurate than previous ones, were obtained at a fraction of the cost, and are the only ones that cover the full range from weak to strong coupling<sup>8</sup> and a large range of anisotropies. Furthermore, we have presented a simple parameterization of our results, eq. (4.6) with  $a_0 = -0.77810$  and  $a_1 = -0.55055$ , that reproduces all data within errors and is consistent with perturbation theory at weak coupling. For lattice spacings of interest in practice we find that the renormalization of the anisotropy is much larger than predicted by one-loop perturbation theory (even when “boosted”). Our results are therefore crucial for future applications.

The errors of our results, about 1% on coarse and less on finer lattices, should also be sufficient for future applications. Since our parameterization incorporates the known one-loop behavior, it is quite clear that the error in an observable due to the remaining small error in  $\xi_0(\xi, g^2)$  will (almost completely) extrapolate away in the continuum limit.<sup>9</sup>

Given these results, the anisotropic Wilson gauge action is as simple to use as the isotropic one. The only thing that is currently missing are accurate determinations of the physical scale (string tension and Sommer scale  $r_0$ ) of the anisotropic actions. This gap should soon be filled, since once the renormalized anisotropy is known, the “regular” static potential (cf. sect. 2) can be determined very accurately. Work on this is in progress.

A number of projects using the anisotropic Wilson action can now start immediately. One example is the study of glueballs in pure gauge theory. It will be interesting to see how much of the improvement seen in glueball studies with anisotropic *improved* actions [12] is due to the anisotropy and how much due to the elimination of (most of) the  $O(a_s^2)$  errors. Another example, as remarked at the end of sect. 4, would be to reconsider high precision thermodynamic studies using our results.

One could also start simulations of heavy quark systems in the quenched approximation. An immediate improvement compared to isotropic studies should be apparent (cf. [10]). However, as mentioned in the introduction, truly reliable and accurate studies of such systems will have to await the non-perturbative  $O(a^0)$  and  $O(a)$  improvement of Wilson-type quark actions on anisotropic lattices: The first (and easier) step is to tune the *bare velocity of light* of the quarks so that the fermion and gauge sectors agree on the renormalized anisotropy. The second step involves the tuning of the temporal and spatial clover coefficients to eliminate  $O(a)$  errors [11].<sup>10</sup>

Finally, since our method is free of most lattice artifacts whose elimination would be very expensive beyond the quenched approximation, the prospects for extending this work to full QCD look good. Of course, simulations for full QCD will be significantly more expensive, not just because the determinant of the quark matrix has to be

---

<sup>8</sup>Preliminary results indicate that the lattice spacing for  $\beta = 5.5$  and  $\xi \geq 2$  is close to 0.3 fm. The range of couplings we covered should therefore be sufficient for all future applications.

<sup>9</sup>We are here referring to the statistical and systematic errors of *our method* of determining  $\xi_0(\xi, g^2)$ ; another legitimate method can of course differ by  $O(a^2)$  terms, which are a priori known to extrapolate away in the continuum limit.

<sup>10</sup>This presumably has some (small) effect on the bare velocity of light, which therefore has to be retuned iteratively with the clover coefficients. We expect this iterative retuning to converge rapidly, if necessary at all.

calculated, but also because one has to tune more bare parameters simultaneously to obtain consistent quark and gauge anisotropies (now the quark parameters feed back into the gauge sector). However, the required tuning might not be as hard as it first sounds.

### **Acknowledgements**

I would like to thank Tim Scheideler for discussions and correspondence, as well as Mark Alford and Urs Heller for comments on the manuscript. This work is supported by DOE grants DE-FG05-85ER25000 and DE-FG05-96ER40979. Most of the computations in this work were performed on the workstation cluster at SCRI; the three simulations on  $N_s = 16$  lattices were performed on the QCDSP supercomputer at SCRI. Two different sets of code were used in this project. One was developed in collaboration with Mark Alford and Peter Lepage, the other is SZIN, a macro-based C package developed at SCRI for QCD simulations on a variety of platforms.

## References

- [1] C.T.H. Davies et al (eds.), LATTICE 97, Nucl. Phys. **B** (Proc. Suppl.) **63** (1998), [hep-lat/9801024](#).
- [2] M. Lüscher et al, Nucl. Phys. **B491** (1997) 323, 344.
- [3] R.G. Edwards, U.M. Heller and T.R. Klassen, Nucl. Phys. **B** (Proc. Suppl.) **63** (1998) 847.
- [4] R.G. Edwards, U.M. Heller and T.R. Klassen, Phys. Rev. Lett. **80** (1998) 3448 ([hep-lat 9711052](#)).
- [5] K. Jansen and R. Sommer, Nucl. Phys. **B** (Proc. Suppl.) **63** (1998) 853.
- [6] G.P. Lepage et al, Phys. Rev. **D46** (1992) 4052.
- [7] A.X. El-Khadra, A.S. Kronfeld and P.B. Mackenzie, Phys. Rev. **D55** (1997) 3933.
- [8] H.D. Trottier, Phys. Rev. **D55** (1997) 6844; N.H. Shakespeare and H.D. Trottier, [hep-lat/9802038](#).
- [9] M. Alford, T.R. Klassen and G.P. Lepage, Nucl. Phys. **B496** (1997) 377.
- [10] M. Alford, T.R. Klassen and G.P. Lepage, Nucl. Phys. **B** (Proc. Suppl.) **53** (1997) 861.
- [11] T.R. Klassen, Nucl. Phys. **B509** (1998) 391.
- [12] C. Morningstar and M. Peardon, Phys. Rev. **D56** (1997) 4043; M. Peardon, Nucl. Phys. **B** (Proc. Suppl.) **63** (1998) 23.
- [13] F. Karsch, Nucl. Phys. **B205** (1982) 285.
- [14] G. Burgers, F. Karsch, A. Nakamura, and I.O. Stamatescu, Nucl. Phys. **B304** (1988) 587.
- [15] M. Alford, T.R. Klassen, G.P. Lepage, C. Morningstar, M. Peardon, and H.D. Trottier, in preparation.
- [16] M. Fujisaki et al (QCDTARO Collaboration), Nucl. Phys. **B** (Proc. Suppl.) **53** (1997) 426.
- [17] J. Engels, F. Karsch and T. Scheideler, Nucl. Phys. **B** (Proc. Suppl.) **63** (1998) 427.
- [18] T. Scheideler, Ph.D. Thesis, Bielefeld, January 1998.
- [19] A.D. Kennedy and B.J. Pendleton, Phys. Lett. **156B** (1985) 393; M. Creutz, Phys. Rev. **D21** (1980) 2308.
- [20] N. Cabibbo and E. Marinari, Phys. Lett. **119B** (1982) 387.

- [21] G. Parisi, R. Petronzio and F. Rapuano, Phys. Lett. **128B** (1983) 418.
- [22] M. García Pérez and P. van Baal, Phys. Lett. **B392** (1997) 163.
- [23] G. Parisi, p. 1531 in: “High Energy Physics – 1980”, L. Durand and L.G. Pondrom (eds.), AIP, New York, 1981; G. Martinelli, G. Parisi and R. Petronzio, Phys. Lett. **100B** (1981) 485.
- [24] G.P. Lepage and P.B. Mackenzie, Phys. Rev. **D48** (1993) 2250.
- [25] J. Engels et al, Phys. Lett. **B252** (1990) 625.
- [26] G. Boyd et al, Nucl. Phys. **B469** (1996) 419.
- [27] J. Engels, F. Karsch and K. Redlich, Nucl. Phys. **B435** (1995) 295.
- [28] P. Pennanen, A.M. Green and C. Michael, Phys. Rev. **D56** (1997) 3903.
- [29] R.G. Edwards, U.M. Heller and T.R. Klassen, Nucl. Phys. **B517** (1998) 377 (hep-lat/9711003).
- [30] J. Engels, F. Karsch and H. Satz, Nucl. Phys. **B205** (1982) 239.
- [31] O. Kaczmarek, Diplom Thesis, Bielefeld, September 1997.